

Stern–Brocot trees in cascades of mixed-mode oscillations and canards in the extended Bonhoeffer–van der Pol and the FitzHugh–Nagumo models of excitable systems

Joana G. Freire ^{a,b}, Jason A.C. Gallas ^{a,b,c,*}

^a Instituto de Física, Universidade Federal do Rio Grande do Sul, 91501-970 Porto Alegre, Brazil

^b Centro de Estruturas Lineares e Combinatórias, Faculdade de Ciências, Universidade de Lisboa, 1649-003 Lisboa, Portugal

^c Departamento de Física, Universidade Federal da Paraíba, 58051-970 João Pessoa, Brazil

ARTICLE INFO

Article history:

Received 18 November 2010

Accepted 8 January 2011

Available online 13 January 2011

Communicated by A.R. Bishop

Keywords:

Mixed-mode oscillations

Stern–Brocot tree

Farey tree

Period-adding

Periodicity hub

Phase diagram

ABSTRACT

We report a systematic two-parameter study of the organization of mixed-mode oscillations and period-adding sequences observed in an extended Bonhoeffer–van der Pol and in a FitzHugh–Nagumo oscillator. For both systems, we construct isospike diagrams and show that the number of spikes of their periodic oscillations are organized in a remarkable hierarchical way, forming a Stern–Brocot tree. The Stern–Brocot tree is more general than the Farey tree. We conjecture the Stern–Brocot tree to also underlie the hierarchical structure of periodic oscillations of other systems supporting mixed-mode oscillations.

© 2011 Elsevier B.V. All rights reserved.

1. Introduction

Mixed-mode oscillation is a ubiquitous phenomenon studied profusely in experiments and models of prototypic dynamical systems in chemistry [1–10], physics [11–15], and neuroscience [16–21]. Mixed-mode oscillations (MMOs) are complex oscillatory patterns consisting of trains of small amplitude oscillations followed by large excursions of relaxation type. For a recent survey about the properties and use of MMOs in several fields see Ref. [22].

Although MMOs have already been observed abundantly, such observations were mostly done by considering the dynamics along one-parameter sections of multidimensional parameter spaces. An exception is an interesting work published recently in this journal by Sekikawa et al. [23]. Among other things, these authors reported two-parameter bifurcation diagrams of the period-doubling bifurcations associated with canards [24] in an extended Bonhoeffer–van der Pol (BVP) oscillator shown schematically in Fig. 1. This system is an extended version of the paradigmatic model of mathematical neuroscience [25] considered by FitzHugh [26] and Nagumo et al. [27].

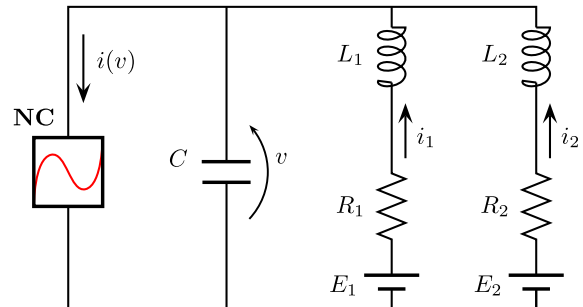


Fig. 1. Schematic representation of the BVP oscillator. NC refers to the nonlinear conductance defined in Eq. (4).

Sekikawa et al. [23] showed that the generation of MMOs and chaos in the BVP model does not occur only in the presence of subcritical Andronov–Hopf bifurcations [24], but may also arise in the supercritical case. Further, by considering bifurcation diagrams, they have shown period-doubling cascades of canards responsible for MMOs and for period-adding sequences to exist in narrow parameter regions where the original canard is observed in the non-extended model.

Our motivation for this work arises from the fact that the period-adding sequences studied by Sekikawa et al. [23] resemble a number of similar sequences observed recently in rather dis-

* Corresponding author at: Instituto de Física, Universidade Federal do Rio Grande do Sul, 91501-970 Porto Alegre, Brazil.

E-mail address: jgallas@if.ufrgs.br (J.A.C. Gallas).

tinct scenarios connected with certain “periodicity hubs” [28–31]. Such hubs are remarkable points responsible for organizing the dynamics around large portions of the parameter space [30]. For us, systems displaying MMs are particularly attractive to investigate and probe details associated with the nature of the intricate reinjections, homoclinic or not, causing periodicity hubs [31] and of certain reinjection mechanisms arising in multiple-timescale systems.

This Letter reports the discovery of a new hierarchical organization of periodic oscillations in the parameter space. Contrary to a common understanding, in two prototypic models we find MMs not to arise structured according to the familiar Farey tree [32] but, instead, in a distinct but equally remarkable organization, forming the so-called Stern–Brocot tree [33,34]. The Stern–Brocot trees are more general than Farey trees and include them as subtrees [35,36]. They may be recognized when contemplating the unfolding of oscillations in two-parameter sections of the control parameter space. Before proceeding, we mention that we also found the Stern–Brocot tree in other popular models of MMs. However, in this Letter we focus in just two models, namely the BVP and the FitzHugh–Nagumo models.

In the next section we review briefly the extended Bonhoeffer–van der Pol oscillator of Sekikawa et al. [23] and define basic notation. In Section 3 we complement results of Sekikawa et al. by presenting high-resolution isospike diagrams showing how the spikes of periodic oscillations auto-organize in parameter space. In Section 4 we present isospike diagrams for the second example, the FitzHugh–Nagumo model, the backbone of the extended Bonhoeffer–van der Pol oscillator. Isospike diagrams for both models display similar hierarchical structures which, however, are more easily visible in the FitzHugh–Nagumo model. In Section 5, we present the Stern–Brocot tree which underlies the hierarchical structure of MMs found for both the extended Bonhoeffer–van der Pol oscillator and the FitzHugh–Nagumo model. Finally, Section 6 summarizes our conclusions.

2. The BVP autonomous oscillator

An important point about the extended Bonhoeffer–van der Pol system is that, rather than being just an abstract set of equations, as stressed by Sekikawa et al., the model may be tested in the laboratory using the circuit in Fig. 1. The equations governing this circuit are [23,37,38]:

$$C \frac{dv}{dt} = i_1 + i_2 - i(v), \quad (1)$$

$$L_1 \frac{di_1}{dt} = -v - r_1 i_1 + E_1, \quad (2)$$

$$L_2 \frac{di_2}{dt} = -v - r_2 i_2 + E_2, \quad (3)$$

where the nonlinear conductance $i(v)$ is given by a cubic characteristic

$$i(v) = -g_1 v + g_3 v^3. \quad (4)$$

In these equations C , L_i , r_i , E_i represent a capacitor, inductances, resistances and sources, respectively. NC denotes the nonlinear conductance governed by Eq. (4). As usual, i_i and v represent currents and voltage, as indicated. By introducing a rescaled time defined by $t = L_1 g_1 \tau$, calling $\beta \equiv \sqrt{g_1/g_3}$, and changing variables and parameters as follows

$$v = \beta x, \quad i_1 = g_1 \beta y, \quad i_2 = g_1 \beta z, \quad (5)$$

$$E_1 = \beta B_0, \quad E_2 = \beta B_1, \quad \varepsilon = C/(L_1 g_1^2), \quad (6)$$

$$k_1 = g_1 r_1, \quad k_2 = g_1 r_2, \quad k_3 = L_1/L_2, \quad (7)$$

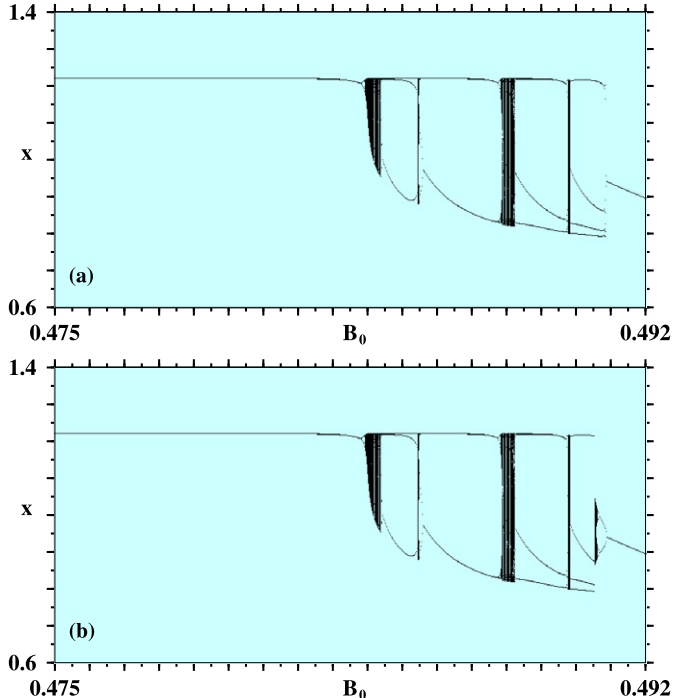


Fig. 2. Bifurcation diagrams illustrating period-adding and the existence of multistability in the right end of the parameter range. (a) Following the attractor from left to right. (b) Following right to left. Here $k_3 = 0.4$.

one may reduce Eqs. (1)–(3) to a simpler form which we will effectively use:

$$\varepsilon \frac{dx}{dt} = x(1-x^2) + y + z, \quad (8)$$

$$\frac{dy}{dt} = -x - k_1 y + B_0, \quad (9)$$

$$\frac{dz}{dt} = k_3(-x - k_2 z + B_1), \quad (10)$$

where, for simplicity, we wrote t instead of τ . This autonomous set of equations defines a dissipative flow governed by a six-dimensional (control) parameter space. Following Sekikawa et al. [23] we set $k_2 = k_1$, $B_1 = B_0$, and fix $k_1 = 0.35$.

Fig. 2 shows typical bifurcation diagrams for Eqs. (8)–(10). The diagram on the top of Fig. 2 was obtained by starting from $B_0 = 0.475$ and “following the attractor” [39] to the right while in the other diagram we started from $B_0 = 0.492$ followed the attractor to the left. They illustrate period-adding sequences and something that will appear more forcefully in the next figures: the presence of multistability for large values of B_0 .

3. Isospike diagrams

In Fig. 3 we present a comparison between phase diagrams obtained by Sekikawa et al. [23] with diagrams computed by us using our in-house software. The diagrams of Sekikawa et al. are shown in the top row. The central row shows our first set of phase diagrams, namely *isospike diagrams*, discriminating with colors parameter domains characterized by periodic oscillations with an identical number of spikes within a period. Such diagrams are a sort of generalized isoperiodic diagrams [40,41]. The isospike diagrams display the 14 lowest periods using the 14 colors indicated by the colorbar, recycling them “mod 14” for higher periods. Black is used to represent parameters leading to non-periodic oscillations, i.e. to chaos, while white marks fixed-points (i.e. constant solutions).

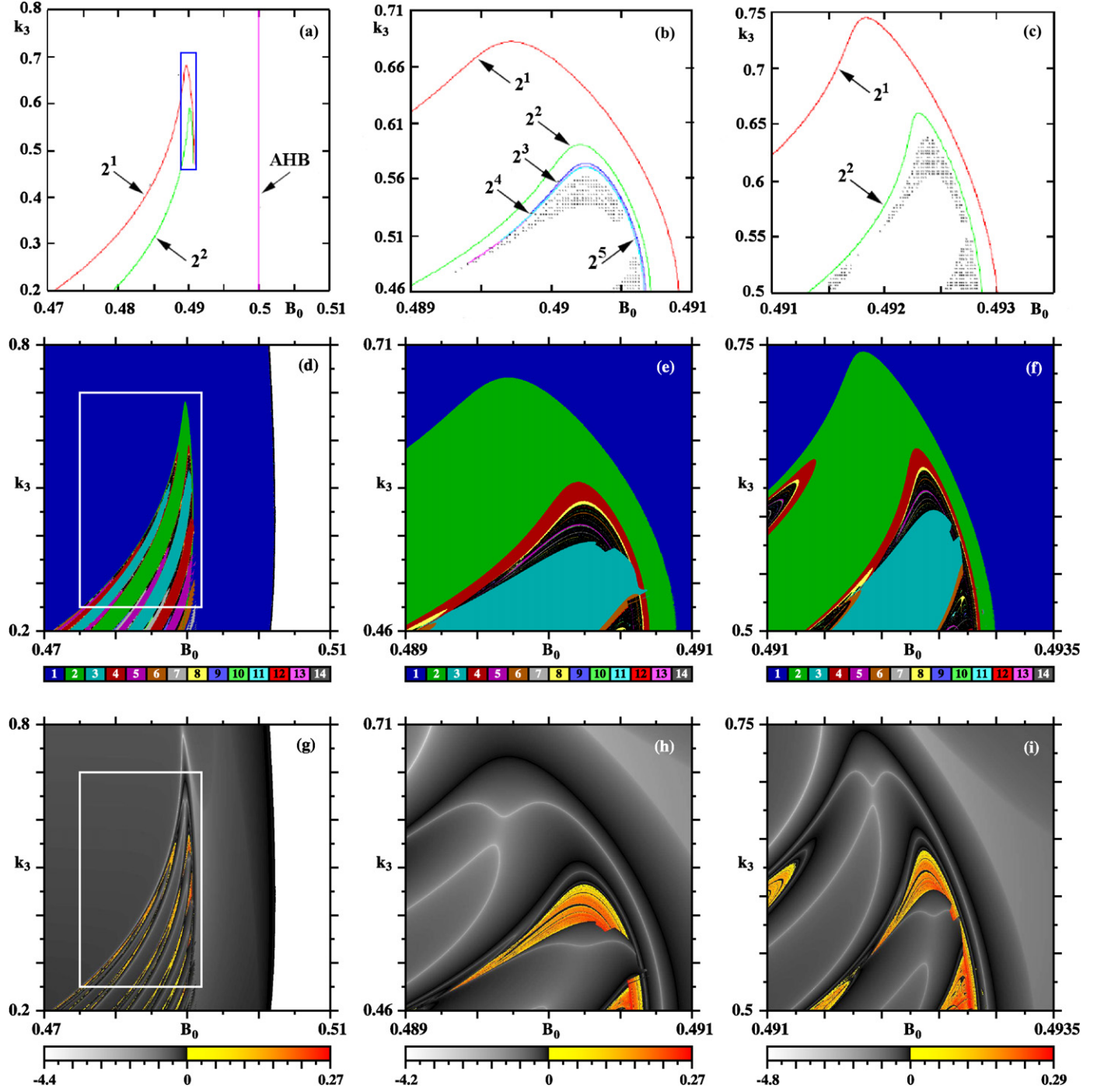


Fig. 3. Top row: Phase diagrams as computed by Sekikawa et al. [23] for Eqs. (8)–(10) for $k_1 = 0.35$ and (a) $\varepsilon = 0.10$; (b) $\varepsilon = 0.10$; (c) $\varepsilon = 0.09$. Numbers indicate beginning of doubling cascades. **Center row:** Isospike diagrams detailing the extension of periodic and chaotic phases. Colors and numbers represent the number of spikes in a period of x , as indicated by the colorbar. The complex region inside the white box in (d) contains a Stern–Brocot tree and is shown magnified in Fig. 4. Note that a second (symmetrical) doubling sequence seen on the left of (f) is missing in (c). **Bottom row:** Lyapunov phase diagrams [30]. Each one of our six diagrams presents results for 800×800 parameter points. (For interpretation of references to color, the reader is referred to the web version of this Letter.)

Comparing the top and central rows in Fig. 3 one easily recognizes that the latter diagrams contain a number of new features. In particular, in Fig. 3(d) it is possible to recognize a dense succession of stripes not present in Fig. 3(a). Such stripes indicate that periodic oscillations with an ever increasing number of spikes exist symmetrically on both sides of the green stripe (which marks parameters leading to periodic oscillations with two spikes in a period). The white box seen in Fig. 3(d) is shown enlarged in Fig. 4, which is discussed in the next section.

The “tip” of the multicolored structure in Fig. 3(d) is shown in Fig. 3(e) where one may recognize the unfolding of the doubling cascade, ending in chaos (black), then a large region characterized by three spikes, then its doubling cascade, followed once again by chaos (black). What Fig. 3(e) does not show is the presence of a symmetrical unfolding of bifurcations on the left of $B_0 = 0.489$. The beginning of such symmetrical unfolding may be recognized in Fig. 3(f) which, however, despite being for $\varepsilon = 0.09$, displays essentially the same structure as that of the tip of Fig. 3(d) (com-

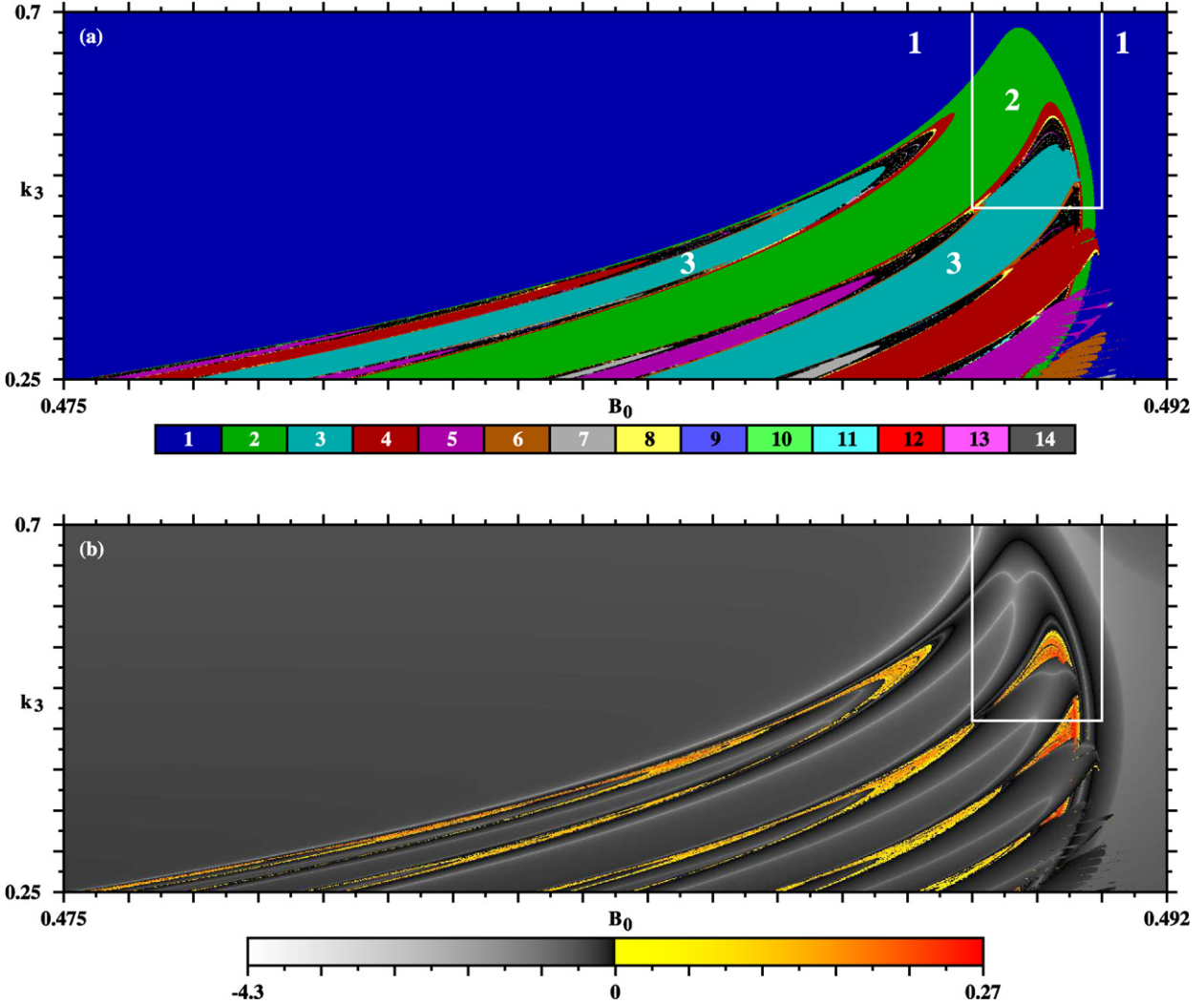


Fig. 4. **Top row:** Isospike diagram displaying the number of spikes measured in one period of x , as indicated by colors and numbers in the colorbar. The organizations of the isospike phases form a Stern–Brocot tree. This panel is a magnification of the box in Fig. 3(d). The white box indicates the parameter region shown in Figs. 3(b) and 3(e). **Bottom row:** The corresponding Lyapunov phase diagram. Each panel presents results for 1200×600 parameter points. (For interpretation of the references to color, the reader is referred to the web version of this Letter.)

puted for $\varepsilon = 0.10$). In other words, Fig. 3(f) may be considered as illustrative of what one sees at the tip of the multicolored structure inside the white box in Fig. 3(d). Note that the dual nature of the unfolding is absent in Fig. 3(c). The full symmetry of the unfolding is shown greatly enlarged in Fig. 4. In Figs. 3(e) and 3(f) it is possible to recognize the presence of multistability in the rightmost boundary of the 3-spike phase, the two-parameter equivalent of the multistability visible in Fig. 2.

Finally, the last row of Fig. 3 shows Lyapunov phase diagrams [30,42,43] for the same three situations. Colors denote parameters leading to chaos, i.e. positive exponents, while darker shadings mark periodicity, as indicated by the color bar. The color scale is linear on both sides of zero but not uniform from negative to positive extrema. From these diagrams it is easy to recognize the location of the chaotic phases, now characterized by positive Lyapunov exponents (not by absence of periodicity as in the central row). The location of the boundaries delimited by Lyapunov exponents coincide with the boundaries shown in the central row, obtained by counting spikes.

Fig. 4 shows with much more detail the isospike phases contained in the white box in Fig. 3(d). In this figure one easily recognizes the effect of multistability on the rightmost part of the diagram, analogously to the differences seen in Fig. 2. The phase

diagrams in Fig. 4 were generated by “following the attractor” [39] from left to right, starting from an arbitrary initial constant. We preferred to expose multistability rather than tune conditions to hide it.

From Fig. 4(a) one recognizes a clear structural organization of the isospike phases and it is natural to ask about how the ordering continues for higher periods. The large blue phase in Fig. 4(a) corresponds to 1-spike oscillations. When decreasing k_3 one meets on the right side of the figure the 2-spikes green phase corresponding to the doubling of the 1-spike oscillations. By further decreasing k_3 one sees that the 2-spikes phase develops two distinct “armpits”, i.e. two symmetric and independent phases characterized by period-doubling cascades that proceed until they accumulate in a chaotic phase, represented in black in Fig. 4(a) [in yellow in Fig. 4(b)]. Although every chaotic phase contains a myriad of smaller isospike phases embedded in it, the next large phases are two 3-spikes phases as indicated in the figure. Each of the 3-spike phases develops its own symmetric pair of armpits. To see how this process proceeds is difficult in the scale of Fig. 4(a). However, the ordering may be recognized by resorting to magnifications of several specific portions of the phase diagram and to bifurcation diagrams (not shown here). The general picture underlying the hierarchical process is the emergence of an infinite cascade of armpit

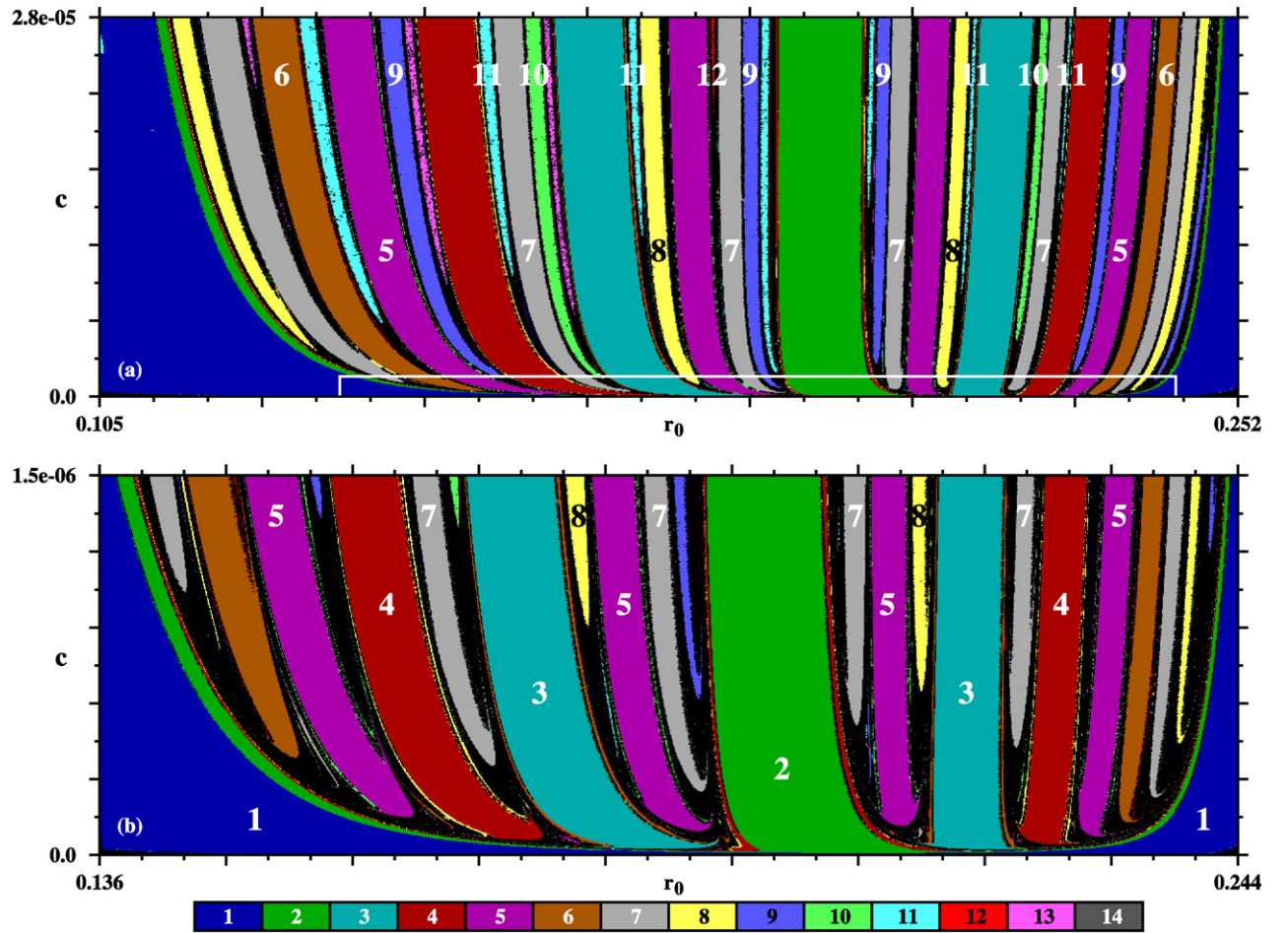


Fig. 5. Stern-Brocot tree observed in isospike diagrams for the FitzHugh–Nagumo model of Eqs. (11)–(13) for a mesh of 1200×600 parameter points. (a) Global view of parameter space. The complete upper sequence should read: (6, 9, 11, 10, 11, 13, 12, 9, 9, 12, 13, 11, 10, 11, 9, 6). The phases corresponding to the numbers inside the three boxes lie outside the scale of the figure. (b) Enlargement of the white box in (a), showing the beginning of the Stern–Brocot tree. Both panels represent spikes as observed in a period of v .

pairs appearing in a definite order, mirror images of each other with respect to the central 2-spikes green domain.

4. FitzHugh–Nagumo oscillator

What is the ordering of the spiking phases in the next level of the isospike diagram described in the previous section? To answer this question, we follow a MMO cascade in a distinct model, which we found to display a more tractable diagram. For such model it will be possible to recognize the unfolding of periodicity from few diagrams, the pair in Fig. 5.

The second model used is the FitzHugh–Nagumo oscillator which, as mentioned earlier, is in fact the backbone of the BVP model. Specifically, we consider the fast-slow dynamical system for which Durham and Moehlis [44] found periodic or chaotic mixed-mode oscillations when controlling the system undergoing a supercritical Hopf bifurcation to be in the canard regime. Their system is [44]

$$\frac{dv}{dt} = -w - v(v - 1)(v - a) + I, \quad (11)$$

$$\frac{dw}{dt} = \epsilon(v - \gamma w), \quad (12)$$

$$\frac{dI}{dt} = c(r_0 - \sqrt{(v - v_i)^2 + (w - w_i)^2}), \quad (13)$$

where $a, c, r_0, \epsilon, \gamma$ are parameters and

$$v_i = \frac{1}{3}(1 + a - \sqrt{1 - a + a^2}), \quad (14)$$

$$w_i = v_i/\gamma. \quad (15)$$

Following Durham and Moehlis [44] we fix $a = 0.1$, $\epsilon = 0.008$, $\gamma = 1$.

Fig. 5 shows phase diagrams for Eqs. (11)–(13) similar to the ones in Figs. 3 and 4. From Fig. 5 it is possible to recognize more easily how sequences of periodic oscillations auto-organize in parameter space, namely the sequence of dominant periods that emerge under the “armpits” as parameter changes. An important fact becomes now clear: bifurcation diagrams involving the variation of a single parameter are not able to catch the subtle unfolding of the MMO cascades. This is so because the several isospiking phases start in positions that cannot be all intersected simultaneously with a line segment.

5. The tree of Stern and Brocot

The correlation between the periodic oscillations progressively observed in parameter space for MMOs is traditionally investigated by establishing a one-to-one correspondence of these oscillations with an ordered set of rational numbers. To do this one normally starts by first establishing a taxonomy for MMOs by introducing a symbol L^s where L and s refer, respectively, to the number of large and small amplitude excursions recorded in the time evolution of one of its variables. A well-known ordering of rationals is generated by assigning to a given pair p/q and p'/q' of ratios

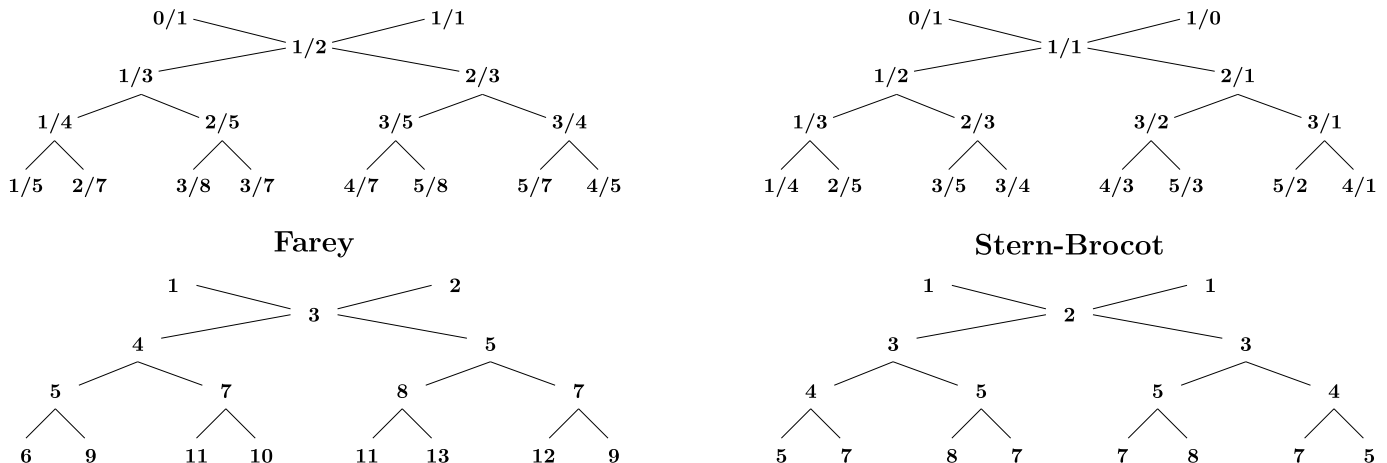


Fig. 6. **Top row:** Schematic representation of the Farey and the Stern–Brocot trees. **Bottom row:** Derived sequences obtained by summing numerator and denominator of the fractions in the Farey and Stern–Brocot trees. The derived sequence obtained from the Stern–Brocot tree reproduces the structure of the cascades in Figs. 3–5.

nals an intermediary “median” rational $(p + p')/(q + q')$. Since the number of spikes in a period is defined by a single integer, not by a rational number, we consider “derived trees” formed by simply summing p and q of known trees used in number theory to represent sequences of rationals. Fig. 6 compares the sequences of rationals as generated by Farey [32] and by Stern–Brocot [35] sequences. Below them we show *sum-trees* derived by simply adding numerators and denominators.

As it is clear from the derived sum-trees in Fig. 6, the spiking ordering of our MMOs does not correspond to the one generated by the Farey tree but is in perfect agreement with the integers of the Stern–Brocot sum-tree. This “good” tree was devised independently in 1858 by Moritz Stern [33] and in 1861 Achille Brocot [34]. Stern was a German mathematician and Brocot was a French clockmaker who used the Stern–Brocot tree to design systems of gears with a gear ratio close to some desired value by finding a ratio of small numbers near that value.

The Stern–Brocot sequence differs from the Farey sequence in two basic ways [35]: it eventually includes all positive rationals, not just the rationals within the interval $[0, 1]$, and at the n -th step all mediants are included, not only the ones with denominator equal to n . The Farey sequence of order n may be found by an in-order traversal of the left subtree of the Stern–Brocot tree, backtracking whenever a number with denominator greater than n is reached. “But we had better not discuss the Farey series any further, because the entire Stern–Brocot tree turns out to be even more interesting.” [35].

As mentioned, the sequences of integers in the derived Stern–Brocot sum-tree coincide with the hierarchical organization of spikes found in Figs. 3–5. Thus, to the *abstract* application in number theory and the nice *practical* application devised originally by Brocot, we now add another “practical” use for the Stern–Brocot tree: the integers in sum-trees extracted from them match exactly the unfolding of spikes observed ordinarily in mixed-mode oscillations.

Two factors are important to identify the Stern–Brocot tree: first, one needs to sweep finely two parameters simultaneously and, second, the tree is observed in isospike diagrams. We find the total number of spikes to be a more reliable indicator than to the large-small L^s labeling that can produce ambiguities when tuning two parameters on a finely spaced mesh. For instance, the attribution of the labels 1^0 and 0^1 is ambiguous from the outset as also is the set of multiple labels possible for sequences of spikes of comparable amplitudes evolving as parameters are changed slightly.

We further remark that while isospike diagrams obtained by using just one of the dynamical variables are easy to obtain and

generally reliable, sometimes the final diagram might depend of the choice of the variable. This is so because the number of spikes of the individual variables governing dynamical systems evolves independently from each other [28]. However, such dependencies may be eliminated by considering the *vector* quantity defined by taking into consideration all components governing the flow. But this extra care is not always necessary. For instance, identical isospike diagrams are obtained by counting spikes from either $x(t)$, or $y(t)$, or $z(t)$, in Eqs. (8)–(10).

6. Conclusions

In summary, we studied the unfolding of cascades of mixed-mode oscillations for two prototypical models of excitable systems. By continuously recording changes in the number of spikes of periodic oscillations when a pair of parameters is tuned simultaneously, we found the number of spikes in periodic oscillations to emerge organized according to a regular tree of integers that is easily derived from a Stern–Brocot tree. Although not yet reported, we already identified the same ordering to be present in a few other standard models displaying MMOs. Therefore, we believe the Stern–Brocot tree to hold great significance for the generic description of the hierarchical structure of oscillations observed routinely in systems supporting mixed-mode scenarios. Since the Farey tree is believed to have been frequently sighted in devil’s staircases generated by MMOs, an enticing challenge seems now to be to recognize Stern–Brocot order in such cascades. Be it as it may, we believe that the nice Stern–Brocot tree will become a major player in the description of periodic oscillations for a large class of nonlinear systems.

Acknowledgements

J.G.F. thanks FCT, Portugal, for a Postdoctoral Fellowship, Grant No. SFRH/BPD/43608/2008 and IF-UFRGS for hospitality. J.A.C.G. is supported by CNPq, Brazil, and by the Air Force Office of Scientific Research, grant FA9550-07-1-0102. All computations were done in the computer clusters of the CESUP-UFRGS.

References

- [1] J. Hudson, M. Hart, D. Marinko, J. Chem. Phys. 71 (1979) 1601.
- [2] J.S. Turner, J.C. Roux, W.D. MacCormick, H.L. Swinney, Phys. Lett. A 85 (1981) 9.
- [3] P. Ibison, S.K. Scott, J. Chem. Soc. Faraday Trans. 86 (1990) 3695.
- [4] V. Petrov, S.K. Scott, K. Showalter, J. Chem. Phys. 97 (1992) 6191.
- [5] K. Krischer, M. Eiswirth, G. Ertl, J. Phys. Chem. 96 (1992) 9161.

- [6] K. Krischer, M. Lübke, M. Eiswirth, W. Wolf, J.L. Hudson, G. Ertl, *Physica D* 62 (1993) 123.
- [7] I.R. Epstein, K. Showalter, *J. Phys. Chem.* 100 (1996) 13132.
- [8] N. Baba, K. Krischer, *Chaos* 18 (2008) 015103.
- [9] K. Kovacs, M. Leda, V.K. Vanag, I.R. Epstein, *J. Phys. Chem. A* 113 (2009) 146.
- [10] L. Yuan, Q. Gao, Y. Zhao, X. Tang, I.R. Epstein, *J. Phys. Chem. A* 114 (2010) 7014.
- [11] For a survey see H.L. Swinney, *Physica D* 7 (1983) 3, and references therein.
- [12] T. Braun, J. Lisboa, J.A.C. Gallas, *Phys. Rev. Lett.* 68 (1992) 2770, and references therein.
- [13] S. Rajesh, G. Ananthakrishna, *Physica D* 140 (2000) 193.
- [14] T. Hayashi, *Phys. Rev. Lett.* 84 (2000) 3334.
- [15] M. Mikikian, M. Cavarroc, L. Couedel, Y. Tessier, L. Boufendi, *Phys. Rev. Lett.* 100 (2008) 225005.
- [16] C.A. Del Negro, C.G. Wilson, R.J. Butera, H. Rigatto, J.C. Smith, *Biophys. J.* 82 (2002) 206.
- [17] G. Medvedev, J.E. Cisternas, *Physica D* 194 (2004) 333.
- [18] A. Kuznetsov, N. Kopell, C. Wilson, *J. Neurophysiol.* 95 (2006) 932.
- [19] J. Rubin, M. Wechselberger, *Chaos* 18 (2008) 015105.
- [20] B. Ermentrout, M. Wechselberger, *SIAM J. Appl. Dyn. Syst.* 8 (2009) 253.
- [21] H. Rotstein, M. Wechselberger, N. Kopell, *SIAM J. Appl. Dyn. Syst.* 7 (2008) 1582.
- [22] M. Brøns, T.J. Kaper, H.G. Rotstein, *Chaos* 18 (2008) 01501.
- [23] M. Sekikawa, N. Inaba, T. Yoshinaga, T. Hikihara, *Phys. Lett. A* 374 (2010) 3745.
- [24] G. Medvedev, Y. Yoo, *Physica D* 228 (2007) 87.
- [25] E.M. Izhikevich, R. FitzHugh, *Scholarpedia* 1 (9) (2006) 1349.
- [26] R. FitzHugh, *Biophysical J.* 1 (1961) 445.
- [27] J. Nagumo, S. Arimoto, S. Yoshizawa, *Proc. IRE.* 50 (1962) 2061.
- [28] C. Bonatto, J.A.C. Gallas, *Phys. Rev. Lett.* 101 (2008) 054101.
- [29] G.M. Ramirez-Avila, J.A.C. Gallas, *Revista Boliviana de Fisica* 14 (2008) 1; G.M. Ramirez-Avila, J.A.C. Gallas, *Phys. Lett. A* 375 (2010) 143.
- [30] J.A.C. Gallas, *Int. J. Bifurc. Chaos* 20 (2010) 197.
- [31] J.G. Freire, J.A.C. Gallas, *Phys. Rev. E* 82 (2010) 037202.
- [32] S.B. Guthery, *A Motif of Mathematics: History and Applications of the Median and the Farey Sequence*, Docent Press, Boston, 2010.
- [33] M.A. Stern, *J. Reine Angew. Math.* 55 (1858) 193.
- [34] A. Brocot, *J. Horlogers Scientifique Pratique* 3 (1861) 186.
- [35] R. Graham, D. Knuth, O. Patashnik, *Concrete Mathematics*, second ed., Addison-Wesley, 1994.
- [36] R. Backhouse, J.F. Ferreira, *Sci. Computer Progr.* 76 (2011), in press, doi:10.1016/j.scico.2010.05.006.
- [37] A.N. Njah, U.E. Vincent, *J. Sound Vibr.* 319 (2009) 41.
- [38] Y. Nishiuchi, T. Ueta, H. Kawakami, *Chaos Sol. Frac.* 27 (2006) 941.
- [39] J.G. Freire, R.J. Field, J.A.C. Gallas, *J. Chem. Phys.* 131 (2009) 044105.
- [40] J.A.C. Gallas, *Phys. Rev. Lett.* 70 (1993) 2714; J.A.C. Gallas, *Physica A* 202 (1994) 196; J.A.C. Gallas, *Appl. Phys. B* 60 (1995) S203.
- [41] J.A.C. Gallas, H.E. Nusse, *J. Econ. Behav. Org.* 29 (1996) 447.
- [42] C. Bonatto, J.C. Garreau, J.A.C. Gallas, *Phys. Rev. Lett.* 95 (2005) 143905.
- [43] M.A. Nascimento, J.A.C. Gallas, H. Varela, *Phys. Chem. Chem. Phys.* 13 (2011) 441, doi:10.1039/C0CP01038C.
- [44] J. Durham, J. Moehlis, *Chaos* 18 (2008) 015110.